



HAL
open science

Pack cementation to prevent the oxidation of CoSb in air at 800 K

Richard Drevet, Lionel Aranda, Nicolas David, Carine Petitjean, Delphine Veys-Renaux, Patrice Berthod

► **To cite this version:**

Richard Drevet, Lionel Aranda, Nicolas David, Carine Petitjean, Delphine Veys-Renaux, et al.. Pack cementation to prevent the oxidation of CoSb in air at 800 K. Surface and Coatings Technology, 2020, 385, pp.125401 -. 10.1016/j.surfcoat.2020.125401 . hal-03489744

HAL Id: hal-03489744

<https://hal.science/hal-03489744>

Submitted on 21 Jul 2022

HAL is a multi-disciplinary open access archive for the deposit and dissemination of scientific research documents, whether they are published or not. The documents may come from teaching and research institutions in France or abroad, or from public or private research centers.

L'archive ouverte pluridisciplinaire **HAL**, est destinée au dépôt et à la diffusion de documents scientifiques de niveau recherche, publiés ou non, émanant des établissements d'enseignement et de recherche français ou étrangers, des laboratoires publics ou privés.



Distributed under a Creative Commons Attribution - NonCommercial 4.0 International License

Pack cementation to prevent the oxidation of CoSb₃ in air at 800 K

Richard DREVET*, Lionel ARANDA, Nicolas DAVID, Carine PETITJEAN, Delphine VEYS-RENAUX, Patrice BERTHOD

Institut Jean Lamour, CNRS - Université de Lorraine, UMR 7198, Campus Artem, allée André Guinier, BP 50840, 54011 Nancy cedex, France.

* corresponding author.

Tel.: +33.372.74.27.29.

e-mail address: richarddrevet@yahoo.fr

Abstract

The skutterudite CoSb₃ is a well-known thermoelectric material widely used to produce electricity from heat. This material is commonly employed under vacuum but in a near future it is expected to be used at high temperatures under oxidative atmospheres, e.g. in air. The lifetime of the material may be affected by the oxidative environment, considerably limiting the use of the thermoelectric equipment. The present research describes the degradation mechanisms of CoSb₃ from oxidation experiments carried out under a flow of synthetic air at 800 K. The skutterudite material is progressively oxidized after 15 h, 50 h, 100 h and 1000 h of treatment, producing three oxides on the CoSb₃ surface (CoSb₂O₄ / CoO·Sb₂O₃, Sb₂O₄ and CoSb₂O₆). These three oxides have different growth kinetics and they are produced in various amounts as a function of the oxidation time.

Next, as a solution for an appropriate oxidation protection, this work explores the chemical vapor deposition (CVD) process named pack cementation to synthesize a protective coating on CoSb_3 . This process produces a surface layer made of aluminum antimonide (AlSb) and cobalt aluminide (Al_9Co_2). The oxidation experiments carried out on the coated CoSb_3 highlight the protective properties of this innovative surface layer. The coating is a protective barrier against oxygen that keeps the CoSb_3 substrate unaffected by the flow of air at 800 K for 1000 hours. Consequently, pack cementation is an efficient process to synthesize a protective surface layer that makes CoSb_3 usable under oxidative environments.

Keywords: skutterudite; oxidation; aluminizing; pack cementation; corrosion; thermoelectric material

1. Introduction

The skutterudite materials are widely studied in the academic and industrial research due to their outstanding thermoelectric properties. They are intensively developed to produce thermoelectric generators able to convert the heat flows into electrical energy [1-3]. The skutterudite materials made of cobalt and antimony are particularly very attractive because of their high electron mobility, high atomic masses, low electrical resistivity and good Seebeck coefficients [4-6]. The most widespread skutterudite material is CoSb_3 , commonly employed at high temperatures under vacuum in space industry [7-9]. This thermoelectric material provides a continuous electrical energy for batteries in satellites and spacecrafts [10]. Since they are powerful electrical energy producers, the skutterudite materials are currently considered as an alternative to the use of fossil fuels on Earth [11-12]. However, under an oxidizing environment such as air at high temperature, they may degrade progressively in service. Ideally, for potential industrial applications, the skutterudite materials have to withstand 1000 hours of exposure in air at 800 K, a relevant temperature found for example in car exhaust gases [12-13]. If this objective is reached, CoSb_3 will be considered as an interesting and powerful material to produce innovative electrical generators. Several research works have described the oxidation behavior of CoSb_3 but mainly at temperatures lower than 800 K. Generally, the oxidation of CoSb_3 induces the formation of a two-part surface layer made of a mixture of antimony oxides outwards and made of a mixture of antimony oxides and cobalt antimonates inwards [14]. This surface layer grows according to a parabolic thickness-time dependence. The growth mechanism occurs in three steps: (i) antimony segregation on the surface, (ii) oxygen penetration into the region of antimony segregation, and (iii) reaction [15]. This oxidation behavior degrades the thermoelectric properties of CoSb_3 and the electrical device durability [16].

In order to lower the impact of oxidation in air at high temperatures, several coating processes have been studied in literature such as magnetron-sputtering or sol-gel process [17-19]. The chemical vapor deposition (CVD) process named pack cementation is well-known to produce protective coatings made of aluminum at the surface of metallic materials [20-22]. Recently we have explored the isothermal section at 600°C of the Al-Co-Sb ternary system to point out the thermodynamic stability of several phases of aluminum and antimony or aluminum and cobalt [23]. These results highlight the relevance of using aluminum pack cementation to produce a surface coating on the skutterudite material CoSb₃. To assess the protection provided by the synthesized surface layer, the current research describes the oxidation behavior of both uncoated and coated CoSb₃ samples under a flow of synthetic air at 800 K for 1000 hours.

2. Materials and Methods

2.1. Synthesis of the skutterudite materials

The CoSb₃ polycrystalline samples were obtained by melting stoichiometric amounts of high purity cobalt (Co, 99.99 %) and antimony (Sb, 99.999 %) at 1373 K for 24 hours in a vitreous-carbon crucible sealed in a quartz tube under partial argon atmosphere. The skutterudite phase is obtained in a second step by cooling down the temperature at 1073 K for a constant annealing for four days. Then, the sample was thoroughly crushed in an agate mortar and the obtained powder is sieved at 36 µm. At last this powder is densified by spark plasma sintering (SPS, Syntex DR SINTER Lab 515S) in graphite dies for 10 minutes at 893 K under 50 MPa. This protocol produces cylindrical samples of 10 mm in diameter and 2 mm in height [24-25].

2.2. Preparation and oxidation of the skutterudite materials

The CoSb₃ skutterudite samples were slightly polished with a 1200 grit SiC paper to remove the surface impurities and ultrasonically cleaned in ethanol. Next, the oxidation of the samples was carried out in a tubular furnace (Carbolite) in which a flow (4 L h⁻¹) of synthetic air, i.e. a mixture of dioxygen (20 % O₂) and dinitrogen (80 % N₂), is continuously injected. The studied temperature to oxidize the samples was 800 K applied for 15 h, 50 h, 100 h and 1000 h.

2.3. Synthesis of the coating

The chemical vapor deposition (CVD) process used to coat the CoSb₃ substrate was pack cementation. Firstly, the surface of the CoSb₃ pellet was polished with a 1200 grit SiC papers and ultrasonically cleaned in ethanol. Then, the pellet was positioned under a dynamic secondary vacuum (10⁻⁶ mbar) inside a sealed silica ampoule that contained a mixture of three powders : 0.60 g of Al (the element to be deposited), 1.40 g of Al₂O₃ (the inert filler powder) and 0.02 g of CrCl₃ (the halide salt activator). These amounts correspond to 0.92 g of powder per cm² of surface of the CoSb₃ sample. The ampoule was annealed in a muffle furnace (Nabertherm) by increasing the temperature with a heating rate of 10 K min⁻¹ until 873 K for 30 min or until 773 K for 120 min. At these temperatures, the atomic diffusions produces a surface layer made of aluminum combined to atoms from the substrate [20-22]. At last, the silica ampoule was air-quenched at room temperature.

2.4. Characterization of the skutterudite materials

The mass variation (Δm) of the oxidized samples was measured with a precision balance (METTLER-TOLEDO). The surface morphology of the samples was observed from secondary

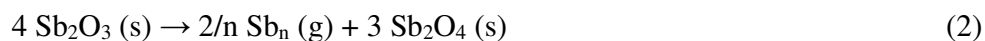
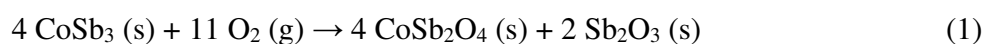
electron (SE) images obtained with a scanning electron microscope (SEM, JEOL JSM 6010LA). The cross-sections were observed from backscattered electron (BSE) images. Moreover, energy dispersive X-ray spectroscopy (EDS) was used to identify the chemical elements inside the surface layer of the oxidized samples and to quantify them from the resulting X-ray microanalysis. In order to get a representative value of these quantifications, three EDS spots were acquired on the whole thickness of the surface layers observed from the cross-section images. The presented values correspond to the average of these triplicate measurements. The crystalline phases of the samples were characterized by X-ray diffraction (XRD) with a Philips X'pert Pro diffractometer using a monochromatic $\text{Cu}_{K\alpha}$ radiation ($\lambda = 0.15406 \text{ nm}$). The patterns were collected from $2\theta = 20^\circ$ to 60° with a step of 0.033° . The phases were identified from the diffraction files provided by the International Centre for Diffraction Data (ICDD).

3. Results and discussion

3.1. Oxidation of the CoSb_3 skutterudite material

The CoSb_3 material has been oxidized under a flow of synthetic air at 800 K for 15 h, 50 h, 100 h and 1000 h. The corresponding surface modifications are presented on the SEM images of **Fig.1**. These SEM observations display the progressive growth of a surface layer with the oxidation time. The cross-section BSE-SEM images of **Fig.2** highlight this surface layer whose thickness increases until 1000 hours of treatment. After 15 h and 50 h of oxidation, only one contrast is noticeable in the newly formed layer. After 100 h and 1000 h of oxidation, several contrasts are clearly visible inside the surface layer, indicating the presence of several different phases [26-27]. The corresponding mass and thickness variations are plotted in **Fig.3**. We can see on these curves that both parameters increase quickly until 100 hours of oxidation. Next, although the thickness of the

layer is still increasing until 1000 hours of oxidation, the mass variation slightly decreases after 1000 hours in comparison with that measured after 100 h of oxidation. In order to understand the oxide layer growth mechanism, the 100 hours oxidation experiment has been reiterated on another CoSb₃ substrate the surface of which has been previously covered by a few nanometers thick gold layer deposited by evaporation process. During the thermal treatment at 800 K, this thin gold layer forms numerous small agglomerates on the surface, clearly observable in white on the cross-section BSE-SEM images of **Fig.4**. The two parts of the surface layer formed during the oxidation treatment are evidently distinguishable on the BSE-SEM images. Their chemical analyzes are carried out from pointed EDS spectra and the corresponding elemental quantifications are reported in **Table 1**. The lower part has grown towards the inside of the CoSb₃ substrate and it is made of oxygen, cobalt and antimony. The upper part has grown towards the outside of the CoSb₃ substrate and it is only made of oxygen and antimony. According to the XRD patterns of **Fig.5**, this oxide layer is mainly composed of the spinel CoSb₂O₄ / CoO·Sb₂O₃, always the major phase whatever the duration of oxidation. From 100 hours of oxidation, Sb₂O₄ appears on the XRD patterns that corresponds to the upper part of the surface oxide layer identified by EDS from the cross-section images of **Fig.2** and **Fig.4**. The oxide Sb₂O₄ is known to be a reaction product obtained in two steps from the unstable oxide Sb₂O₃ according to reaction (1) and reaction (2) [28-29]:



The solid oxidation products Sb₂O₄ (s) is formed at the surface of the oxidized CoSb₃ together with volatile species evaporated just after being formed [29-30]. The more Sb₂O₄ (s) is formed, the more

some elements from the substrate are evaporated. These oxidation reactions explain why the mass variation decreases after 1000 hours of oxidation whereas the oxide layer thickness is still increasing at the surface of the CoSb₃ substrate. At last, the XRD patterns reveal that another oxide (CoSb₂O₆) starts to appear from 100 hours of treatment and becomes clearly noticeable after 1000 hours of oxidation. This phase is positioned at the interface between the two oxides previously presented (CoSb₂O₄ / CoO·Sb₂O₃ and Sb₂O₄). The formation of CoSb₂O₆ takes place after reaction (1) according to reaction (3) [30-31]:



This reaction suggests that some oxygen diffuses through the upper oxide layer (Sb₂O₄) to reach the lower oxide layer (CoSb₂O₄) to react with it. Another explanation provided by Godlewska *et al.* indicates that the phase CoSb₂O₆ appears at the later stages of the oxidation process as a result of a secondary reaction between Sb₂O₄ and CoSb₂O₄ at their interface [28].

Consequently, these results clearly highlight the degradation of the CoSb₃ material under a flow of air at 800 K. The surface protection of this material is essential for any industrial applications in air.

3.2. Aluminizing of the CoSb₃ skutterudite material

The CVD process named pack cementation is used to aluminize two CoSb₃ substrates in two different experimental conditions, one at 773 K for 120 minutes and the other one at 873 K for 30 minutes. The mass of both CoSb₃ samples increases during the deposition process, $\Delta m = +0.86 \text{ mg cm}^{-2}$ and $\Delta m = +1.37 \text{ mg cm}^{-2}$, respectively. The corresponding surface morphologies obtained after deposition are observed on the SEM images of **Fig.6**. In both cases, a dense rough layer is

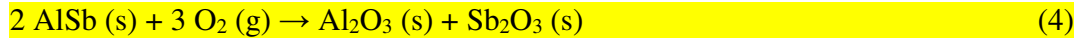
produced at the surface of the CoSb_3 substrate. Indeed, during the pack cementation process, the coating is synthesized by atomic diffusions at the surface of the CoSb_3 substrate. The aluminum atoms react with cobalt and antimony atoms to produce a coating at the surface of the material, keeping the initial topography of the substrate [20-22]. The cross-section BSE-SEM images of Fig.7 and Fig.8 indicate that the thickness of the coatings is 8 μm and 13 μm , respectively. The X-ray maps and the EDS spectra show that these surface coatings are made of aluminum, cobalt and antimony. The corresponding elemental quantifications are reported in Table 1. Both samples show higher amounts of aluminum at the upper part of the coating (spectrum #1) than at the interface with the substrate (spectrum #2). Cobalt is homogeneously distributed inside the coating whereas the amount of antimony is more important close to the substrate. This behavior may suggest that antimony has formed volatile halides by reacting with the halide salt activator present in the pack (CrCl_3) [21]. The EDS analyzes carried out inside the substrates are homogeneous with characteristic quantifications of CoSb_3 . The XRD patterns of Fig.9 reveal that the two synthesized coatings are similarly composed of two crystalline phases. In both cases, the phase AlSb is the major one and the phase Al_9Co_2 is the minor one. From a thermodynamic point of view, the occurrence of only binary phases without any ternary phase has been justified by the description of the diffusion pathway of Al inside CoSb_3 on the isothermal section of the Al-Co-Sb ternary system [23]. Moreover, the isothermal section shows that the thermodynamic equilibrium exists between AlSb and CoSb_3 justifying why AlSb is firstly formed during the pack cementation process. As well, the thermodynamic equilibrium also exists between AlSb and Al_9Co_2 but with no possible equilibrium between Al_9Co_2 and CoSb_3 [23]. This assumption means that the formation of Al_9Co_2 occurs during a second step only inside the AlSb layer with no contact with CoSb_3 . These thermodynamics information implies that during the process the aluminum atoms enter the CoSb_3 structure and firstly react with antimony to form AlSb . This reaction induces the formation of

intermediate compounds such as CoSb_2 or CoSb that progressively insulate cobalt in the structure. Then, during a second step, cobalt inside the surface layer reacts with aluminum to produce Al_9Co_2 certainly promoted by some intermediate compounds such as AlCo , Al_5Co_2 , Al_3Co , $\text{Al}_{13}\text{Co}_4$ [23]. Nonetheless, the amount of Al_9Co_2 is very low and hardly distinguishable from the cross-section BSE-SEM images of **Fig.7** and **Fig.8** although the XRD patterns of **Fig.9** evidence it inside the surface layer. Then, the pack cementation process is a powerful process to produce a surface coating on CoSb_3 the protection properties of which have to be assessed from oxidation experiments.

3.3. Oxidation of the aluminized CoSb_3 skutterudite materials

The results presented in **Fig.10** and **Fig.11** show the cross-section SEM images of the aluminized CoSb_3 substrates after oxidation under a flow of synthetic air at 800 K for 1000 h. The thickness of the surface layer of CoSb_3 aluminized at 773 K increases from 8 μm to 12 μm during the oxidation treatment at 800 K (**Fig.10**). The corresponding mass variation is $\Delta m = + 0.05 \text{ mg cm}^{-2}$. This behavior suggests that the aluminum diffusion continues during the oxidation at 800 K, a temperature upper than that used to aluminize this CoSb_3 sample. On the other hand the thickness of the surface layer of CoSb_3 aluminized at 873 K remains constant during the oxidation treatment at 800 K (**Fig.11**) but this sample shows a higher mass variation $\Delta m = + 0.19 \text{ mg cm}^{-2}$. The different behaviors observed for both samples can be attributed to the two different temperatures used for the pack cementation process that induce two different surface layer thicknesses. The X-ray maps and EDS spectra indicate that these two surface layers are made of oxygen, aluminum, cobalt and antimony. The quantitative analyzes of these four elements are reported in **Table 1**. For both samples, the amounts of oxygen and aluminum are higher in the upper part of the coating (spectrum #1) in comparison with the area close to the interface with the substrate (spectrum #2). The amount

of cobalt is low but homogeneously distributed inside the coating whereas the amount of antimony is higher in the area close to the substrate in comparison with the top area of the coating. The EDS analyzes carried out inside the substrates are homogeneous with characteristic quantifications of CoSb_3 . The X-ray maps show that the whole thickness of the coatings are oxidized with no oxygen detected inside the CoSb_3 substrates. These results highlight the great affinity of the surface layer with oxygen, meaning that the synthesized coating is an efficient barrier against oxygen diffusion that provides an appropriate oxidation protection to CoSb_3 . The corresponding XRD patterns are displayed in **Fig.12**. The signal from AlSb , the main crystalline phase of the coating, is still observable after 1000 h of oxidation at 800 K. However, both XRD patterns include the signal from the CoSb_3 substrate, even for the sample whose surface layer thickness has increased during the oxidation treatment. This observation means that the incident X-rays beam penetrates more deeply the sample certainly because the density of the surface layer has been lowered by the oxidation process [32-33]. The XRD patterns also highlight that no structural change of CoSb_3 occurs during the treatment. On the other hand, one of the oxidized samples also reveal the presence of some alumina ($\alpha\text{-Al}_2\text{O}_3$) meaning that a portion of the formed oxides has been crystallized (**Fig.12b**). The corresponding signal is quite low although oxygen is homogeneously distributed on the X-ray maps of **Fig.10** and **Fig.11** with an average amount upper than 40 at.% (**Table 1**). Indeed, the main crystalline phase of the surface layer is AlSb constituted by aluminum and antimony, two chemical elements particularly well-known for their high affinity with oxygen [34-35]. Sherohman *et al.* have described the oxidation process of AlSb in air in two steps [36]: an initial rapid formation of an oxidized amorphous layer, followed by the continuous oxidation throughout the AlSb material that produces Al_2O_3 and Sb_2O_3 according to reaction (4):



Any deviation from stoichiometry brought by non-equivalent oxidation would produce some Al or Sb. They may promote the formation of hydroxide or hydride compounds such as Al(OH)_3 or SbH_3 that are known for their instability at high temperatures [37-38]. These compounds are easily decomposed from 500 K, producing aluminum oxides (Al_2O_3) and antimony oxides (Sb_2O_3 , Sb_2O_4 , and Sb_2O_5) [39-41]. The volatilization of these unstable compounds can occur during the oxidation treatment, inducing the disruption of the oxidized layer [42]. In our experiments the mechanical stability of the layer is preserved during the oxidation treatment but longer oxidation durations may partially destroy the surface layer [2].

However, our experimental results have clearly evidenced the protection property of the synthesized biphasic coating under air environment at 800 K for 1000 h. The aluminized surface layer acts as a protecting barrier for the CoSb_3 skutterudite material, avoiding any oxygen penetration. The initially targeted objective is then accomplished, making this innovative system interesting and a potential powerful energy producer for many industrial applications.

4. Conclusions

The present research has explored the oxidation behavior of the skutterudite material CoSb_3 under a flow of air at 800 K for 15 h, 50 h, 100 h and 1000 h. The growth of a surface oxide layer has been observed for 1000 h of treatment. This oxide layer is made of three phases. The spinel oxide $\text{CoSb}_2\text{O}_4 / \text{CoO} \cdot \text{Sb}_2\text{O}_3$ grows inwards the substrate and the two oxides Sb_2O_4 and CoSb_2O_6 grow outwards the substrate. In order to prevent the oxidation of CoSb_3 , a protective surface coating has been synthesized by the CVD process named aluminum pack cementation. The synthesis has been

experimented in two conditions, one at 873 K for 30 min or another one at 773 K for 120 min. In both conditions, the obtained biphasic coating is made of AlSb and Al₉Co₂. The oxidation of the coated CoSb₃ under a flow of air at 800 K for 1000 hours has demonstrated the protection properties of this innovative coating that keeps CoSb₃ unaffected by oxygen. Consequently, this coating is a powerful and efficient protection barrier that makes the coated CoSb₃ skutterudite material an interesting device usable for industrial applications under oxidizing environments.

Acknowledgements

The French National Research Agency (ANR) is gratefully acknowledged for the financial support of the Nanoskut project (ANR-12-PRGE-0008-01).

5. References

- [1] M. Rull-Bravo, A. Moure, J.F. Fernandez, M. Martin-Gonzalez, Skutterudites as thermoelectric materials: revisited, *RSC Adv.* 5 (2015) 41653-41667.
- [2] R. Drevet, L. Aranda, C. Petitjean, N. David, D. Veys-Renaux, P. Berthod, Oxidation Behavior of the Skutterudite Material $Ce_{0.75}Fe_3CoSb_{12}$, *Oxid. Met.* 91 (2019) 767-779.
- [3] G. Rogl, P. Rogl, Skutterudites, a most promising group of thermoelectric materials, *Curr. Opin. Green Sustain. Chem.* 4 (2017) 50-57.
- [4] R. Guo, X. Wang, B. Huang, 2015. Thermal conductivity of skutterudite $CoSb_3$ from first principles: Substitution and nanoengineering effects. *Sci. Rep.* 5, 7806.
- [5] J.Q. Guo, H.Y. Geng, T. Ochi, S. Suzuki, M. Kikuchi, Y. Yamaguchi, S. Ito, Development of skutterudite thermoelectric materials and modules, *J. Electron. Mater.* 41 (2012) 1036-1042.
- [6] L. Shi, X. Huang, M. Gu, L. Chen, Interfacial structure and stability in Ni/SKD/Ti/Ni skutterudite thermoelements, *Surf. Coat. Technol.* 285 (2016) 312-317.
- [7] S. Zhang, S. Xu, H. Gao, Q. Lu, T. Lin, P. He, H. Geng, Characterization of multiple-filled skutterudites with high thermoelectric performance, *Journal of Alloys and Compounds* 814 (2020) article # 152272.
- [8] Y. Lei, W. Gao, R. Zheng, Y. Li, R. Wan, W. Chen, L. Ma, H. Zhou, P.K. Chu, Rapid synthesis, microstructure, and thermoelectric properties of skutterudites, *Journal of Alloys and Compounds* 806 (2019) 537-542.
- [9] D. Sivaprahasam, S.B. Chandrasekhar, S. Kashyap, Ashutosh Kumar, R. Gopalan, Thermal conductivity of nanostructured $Fe_{0.04}Co_{0.96}Sb_3$ skutterudite, *Materials Letters* 252 (2019) 231-234.
- [10] W. Liu, Q. Jie, H.S. Kim, Z. Ren, Current progress and future challenges in thermoelectric power generation: From materials to devices, *Acta Mater.* 87 (2015) 357-376.

- [11] L.E. Bell, Colling, heating, generating power, and recovering waste heat with thermoelectric systems, *Science* 321 (2008) 1457-1461.
- [12] V. Andrei, K. Bethke, K. Rademann, Thermoelectricity in the context of renewable energy sources: joining forces instead of competing, *Energy Environ. Sci.* 9 (2016) 1528-1532.
- [13] R. Kühn, O. Koeppen, P. Schulze, D. Jänsch, Comparison between a Plate and a Tube Bundle Geometry of a Simulated Thermoelectric Generator in the Exhaust Gas System of a Vehicle, *Mater. Today proc.* 2 (2015) 761-769.
- [14] V. Savchuk, A. Boulouz, S. Chakraborty, J. Schumann, H. Vinzelberg, Transport and structural properties of binary skutterudite CoSb_3 thin films grown by DC magnetron sputtering technique, *J. Appl. Phys.* 92 (2002) 5319-5326.
- [15] R. Hara, S. Inoue, H.T. Kaibe, S. Sano, Aging effect of large-size n-type CoSb_3 prepared by spark plasma sintering, *J. Alloys Compd* 349 (2003) 297-301.
- [16] Y.S. Park, T. Thompson, Y. Kim, J.R. Salvador, J.S. Sakamoto, Protective enamel coating for n- and p-type skutterudite thermoelectric materials, *J. Mater. Sci.* 50 (2015) 1500-1512.
- [17] E. Godlewska, K. Zawadzka, K. Mars, R. Mania, K. Wojciechowski, A. Opoka, Protective Properties of Magnetron-Sputtered Cr-Si Layers on CoSb_3 , *Oxid. Met.* 74 (2010) 205-213.
- [18] D. Zhao, M. Zuo, Z. Wang, X. Teng, H. Geng, Protective properties of magnetron-sputtered Ti coating on CoSb_3 thermoelectric material, *Appl. Surf. Sci.* 305 (2014) 86-92.
- [19] H. Dong, X. Li, X. Huang, Y. Zhou, W. Jiang, L. Chen, Improved oxidation resistance of thermoelectric skutterudites coated with composite glass, *Ceram. Int.* 39 (2013) 4551-4557.
- [20] X. Xiang, X. Wang, G. Zhang, T. Tang, X. Lai, Preparation technique and alloying effect of aluminide coatings as tritium permeation barriers : A review, *International Journal of Hydrogen Energy* 40 (2015) 3697-3707.

- [21] R. Mévrel, C. Duret, R. Pichoir, Pack cementation processes, *Journal Materials Science and Technology* 2 (1986) 201-206.
- [22] Z.D. Xiang, P.K. Datta, Relationship between pack chemistry and aluminide coating formation for low-temperature aluminisation of alloy steels, *Acta Mater.* 54 (2006) 4453-4463.
- [23] R. Drevet, C. Petitjean, N. David, L. Aranda, D. Veys-Renaux, P. Berthod, Aluminizing by pack cementation to protect CoSb_3 from oxidation, *Mater. Chem. Phys.* 241 (2020) 122417.
- [24] E. Alleno, L. Chen, C. Chubilleau, B. Lenoir, O. Rouleau, M.F. Trichet, B. Villeroy, Thermal Conductivity Reduction in CoSb_3 - CeO_2 Nanocomposites, *J. Electron. Mater.* 39 (2010) 1966-1970.
- [25] M. Benyahia, V. Ohorodniichuk, E. Leroy, A. Dauscher, B. Lenoir, E. Alleno, High thermoelectric figure of merit in mesostructured $\text{In}_{0.25}\text{Co}_4\text{Sb}_{12}$ *n*-type skutterudite, *J. Alloys Compd* 735 (2018) 1096-1104.
- [26] F. Timischl, N. Inoue, Increasing compositional backscattered electron contrast in scanning electron microscopy, *Ultramicroscopy* 186 (2018) 82-93.
- [27] J. Cazaux, N. Kuwano, K. Sato, Backscattered electron imaging at low emerging angles: A physical approach to contrast in LVSEM, *Ultramicroscopy* 135 (2013) 43-49.
- [28] E. Godlewska, K. Zawadzka, A. Adamczyk, M. Mitoraj, K. Mars, Degradation of CoSb_3 in Air at Elevated Temperatures, *Oxid. Met.* 74 (2010) 113-124.
- [29] N.A. Asryan, A.S. Alikhanyan, G.D. Nipan, p-T-x Phase Diagram of the Sb-O System, *Inorg. Mater.* 40 (2004) 626-631.
- [30] J. Leszczynski, K.T. Wojciechowski, A.L. Malecki, Studies on thermal decomposition and oxidation of CoSb_3 , *J. Therm. Anal. Calorim.* 105 (2011) 211-222.
- [31] K. Zawadzka, E. Godlewska, K. Mars, M. Nocun, A. Kryształ, A. Czyrska-Filemonowicz, Enhancement of oxidation resistance of CoSb_3 thermoelectric material by glass coating, *Mater. Des.* 119 (2017) 65-75.

- [32] L.G. Parratt, Surface Studies of Solids by Total Reflection of X-Rays, Phys. Rev. 95 (1954) 359-369.
- [33] Z.H. Kalman, L.A. Johnson, J.B. Wachtman, Density determination of thin coatings by X-ray methods, J. Am. Ceram. Soc. 72 (1989) 1170-1174.
- [34] J. Nakata, T. Shibata, Y. Nanishi, M. Fujimoto, Suppression of AlSb oxidation with hydrocarbon passivation layer induced by MeV-He⁺ irradiation, J. Appl. Phys. 76 (1994) 2078-2085.
- [35] A.J. Rosenberg, The oxidation of intermetallic compounds-III. The room-temperature oxidation of A^{III}B^V compounds, J. Phys. Chem. Solids 14 (1960) 175-180.
- [36] J.W. Sherohman, J.H. Yee, A.W. Coombs, K.J.J. Wu, 2012. Thermal oxidation of single crystal aluminum antimonide and materials having the same. US Patent Application Publication, US8338916B2.
- [37] A.D.V. Souza, C.C. Arruda, L. Fernandes, M.L.P. Antunes, P.K. Kiyohara, R. Salomão, Characterization of aluminum hydroxide (Al(OH)₃) for use as a porogenic agent in castable ceramics, J. Europ. Ceram. Soc. 35 (2015) 803-812.
- [38] E. Haffer, D. Schmidt, P. Freimann, W. Gerwinski, Simultaneous determination of germanium, arsenic, tin and antimony with total-reflection X-ray fluorescence spectrometry using the hydride generation technique for matrix separation—first steps in the development of a new application, Spectrochim. Acta B 52 (1997) 935-944.
- [39] F.W.O. Da Silva, C. Raisin, M. Nouaoura, L. Lassabatère, Auger and electron energy loss spectroscopies study of the oxidation of AlSb(001) thin films grown by molecular beam epitaxy, Thin Solid Films 200 (1991) 33-48.
- [40] S. Jakschik, U. Schroeder, T. Hecht, M. Gutsche, H. Seidl, J.W. Bartha, Crystallization behavior of thin ALD-Al₂O₃ films, Thin Solid Films 425 (2003) 216-220.

[41] R.G. Orman, D. Holland, Thermal phase transitions in antimony (III) oxides, *J. Solid State Chem.* 180 (2007) 2587-2596.

[42] T. Karlsson, C. Forsgren, B.M. Steenari, Recovery of antimony: A laboratory study on the thermal decomposition and carbothermal reduction of Sb(III), Bi(III), Zn(II) oxides, and antimony compounds from metal oxide varistors, *J. Sustain. Metall.* 4 (2018) 194-204.

Figures caption

Fig.1. SEM images of the CoSb₃ surface after oxidation in air at 800 K for (a) 15 h, (b) 50 h, (c) 100 h and (d) 1000 h.

Fig.2. Cross-sections SEM images (BSE) of CoSb₃ after oxidation in air at 800 K for (a) 15 h, (b) 50 h, (c) 100 h and (d) 1000 h.

Fig.3. Mass and thickness evolutions of CoSb₃ as a function of oxidation time in air at 800 K.

Fig.4. Cross-section SEM image (BSE) and EDS spectra of CoSb₃ after oxidation in air at 800 K for 100 h.

Fig.5. XRD patterns of CoSb₃ as a function of oxidation time in air at 800 K.

Fig.6. SEM images of the CoSb₃ surface after aluminizing by CVD (a) at 773 K for 120 minutes and (b) at 873 K for 30 minutes.

Fig.7. SEM images, EDS characterization and X-ray maps of the cross-section of the CoSb₃ surface after aluminizing by CVD at 773 K for 120 minutes.

Fig.8. SEM images, EDS characterization and X-ray maps of the cross-section of the CoSb₃ surface after aluminizing by CVD at 873 K for 30 minutes. Reprinted from Ref. [23] with kind permission from Elsevier.

Fig.9. XRD patterns of the CoSb₃ surface after aluminizing by CVD (a) at 773 K for 120 minutes and (b) at 873 K for 30 minutes.

Fig.10. SEM images, EDS characterization and X-ray maps of the cross-section obtained after oxidation at 800 K for 1000 hours of CoSb₃ aluminized at 773 K for 120 minutes.

Fig.11. SEM images, EDS characterization and X-ray maps of the cross-section obtained after oxidation at 800 K for 1000 hours of CoSb₃ aluminized at 873 K for 30 minutes. Reprinted from Ref. [23] with kind permission from Elsevier.

Fig.12. XRD patterns after oxidation at 800 K for 1000 hours of the aluminized CoSb₃ surface obtained (a) at 773 K for 120 minutes and (b) at 873 K for 30 minutes.

Fig.1

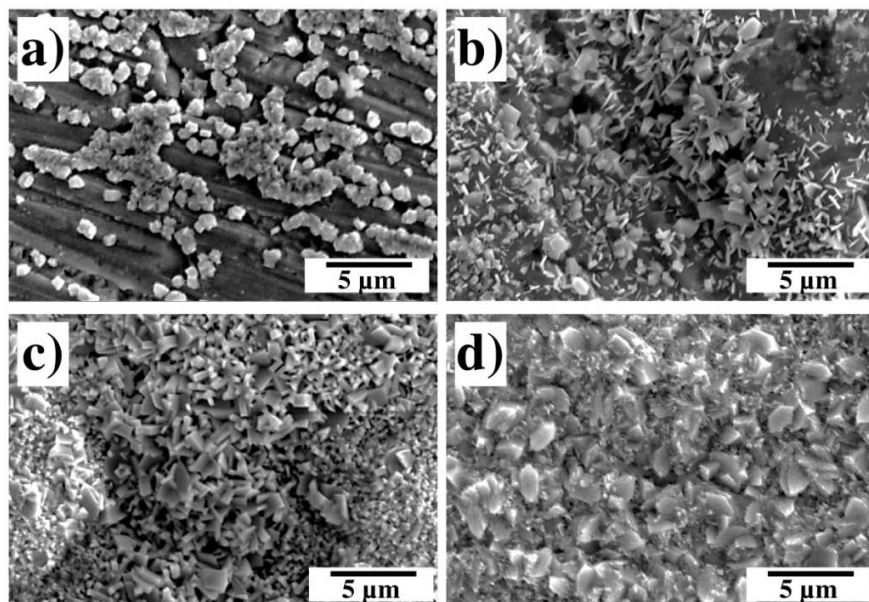


Fig.2

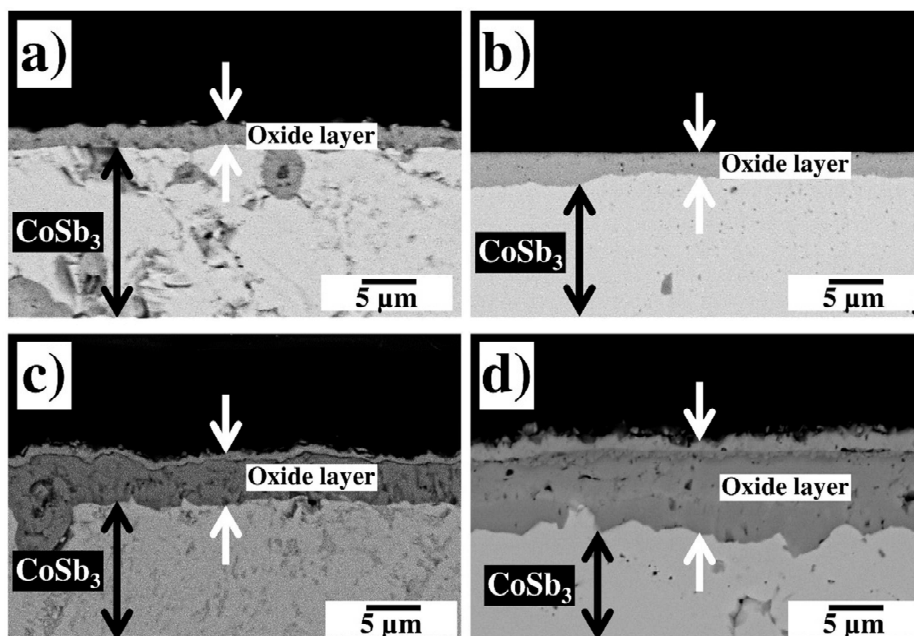


Fig.3

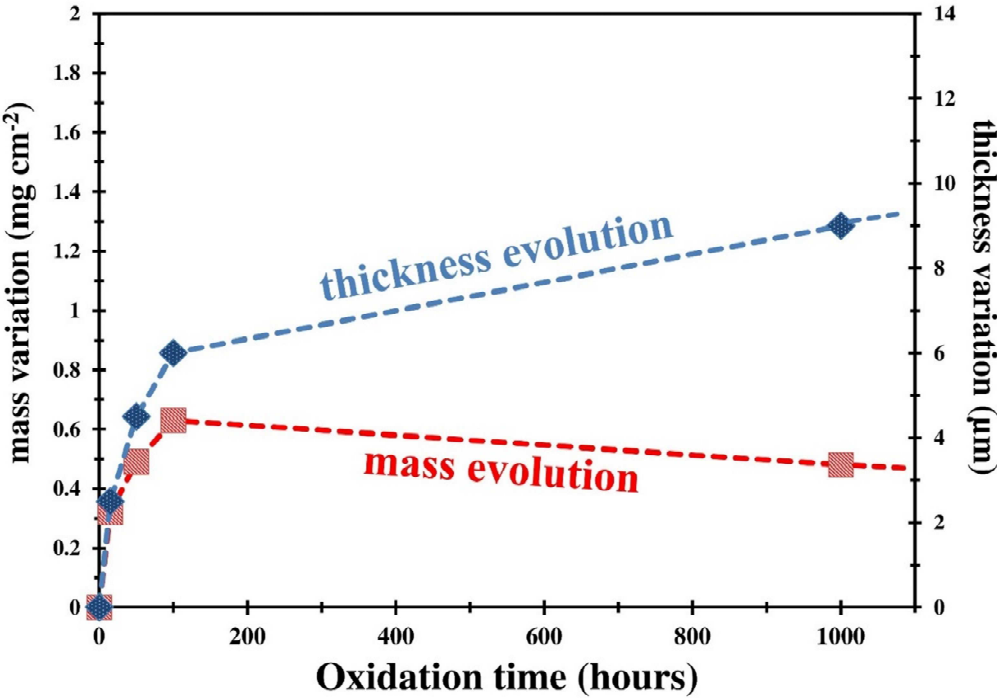


Fig.4

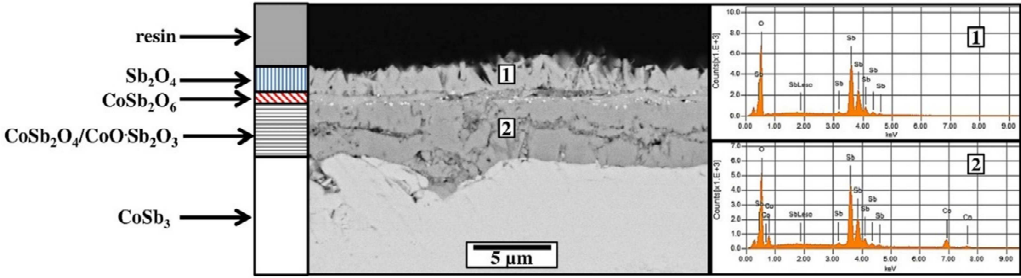


Fig.5

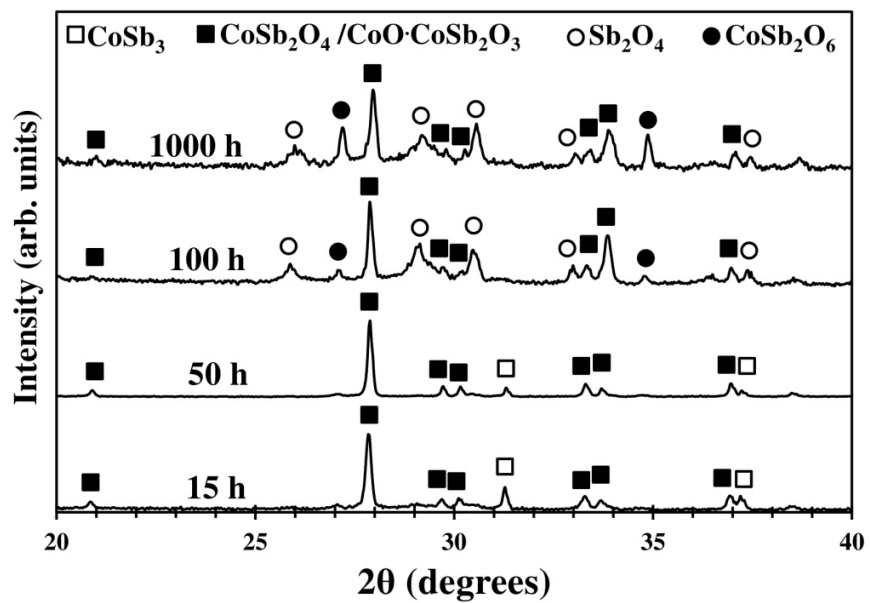


Fig.6

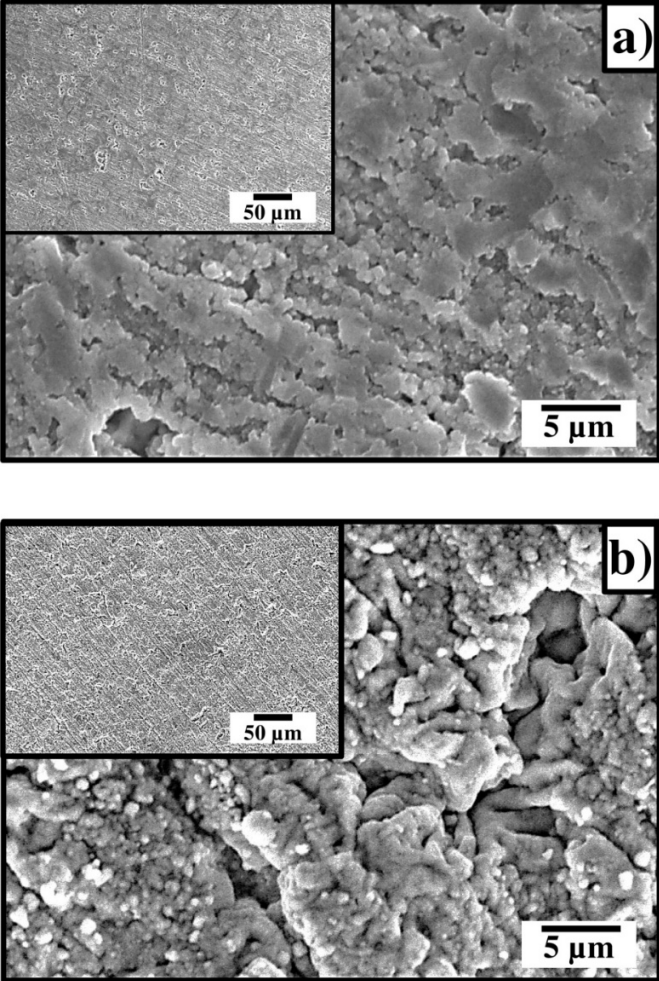


Fig.7

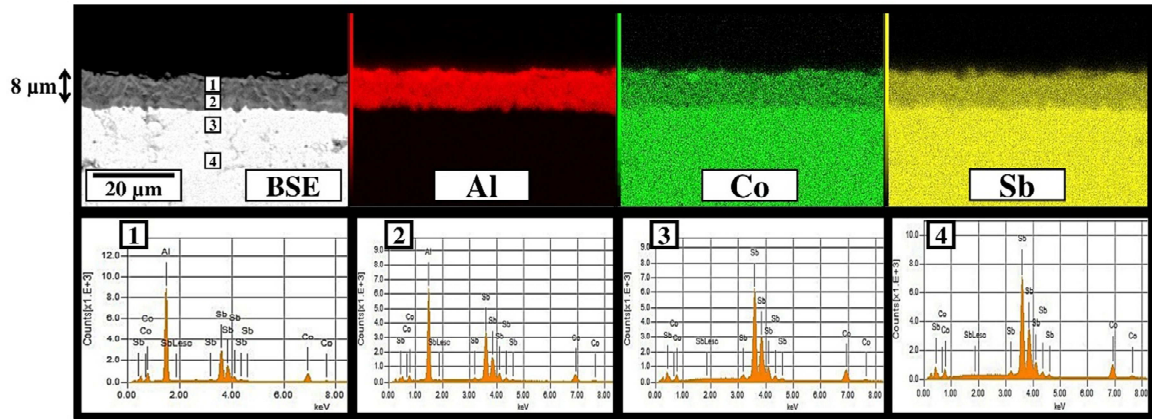


Fig.8

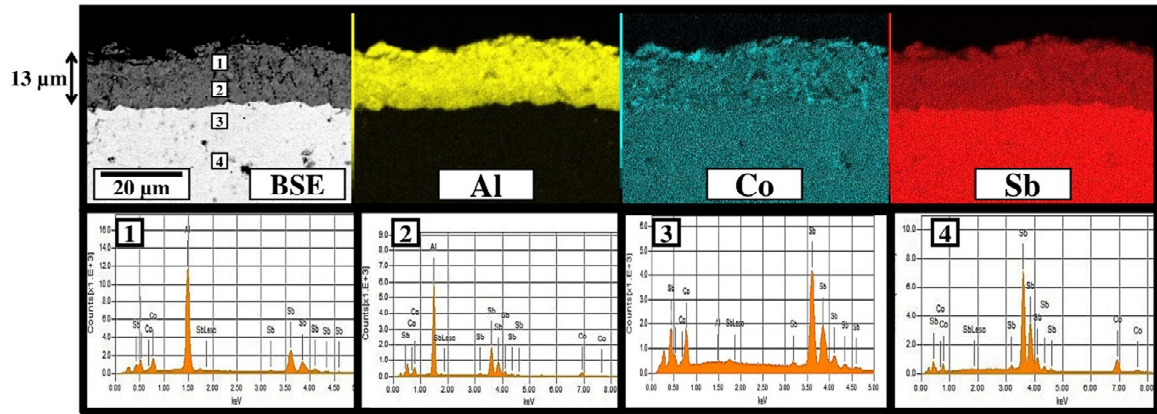


Fig.9

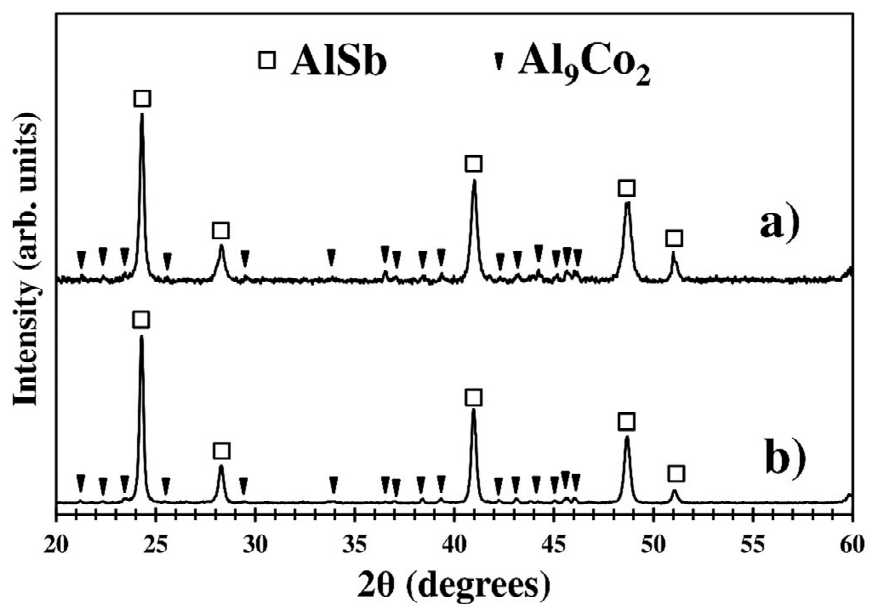


Fig.10

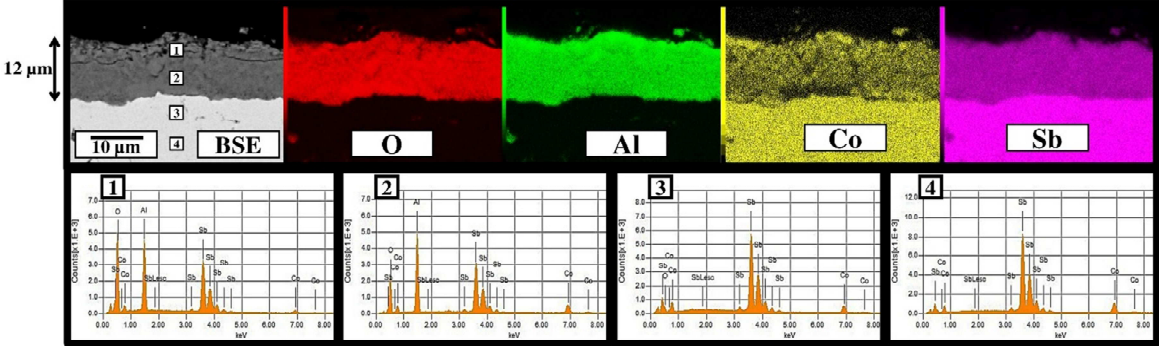


Fig.11

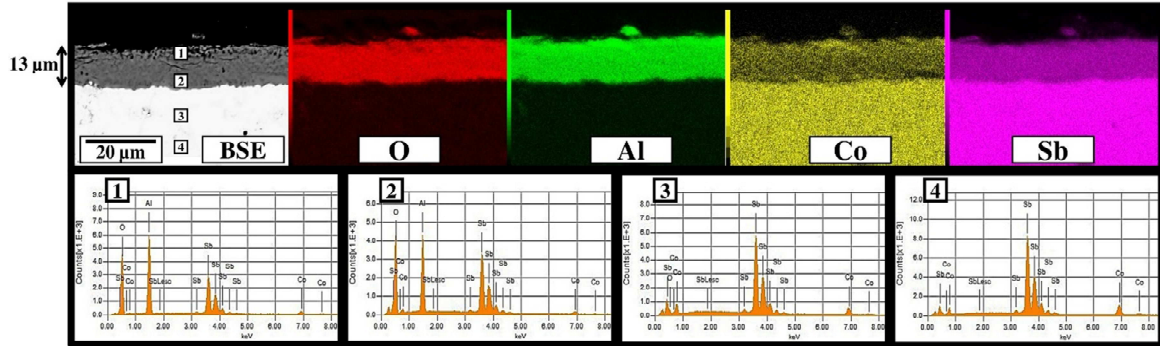


Fig.12

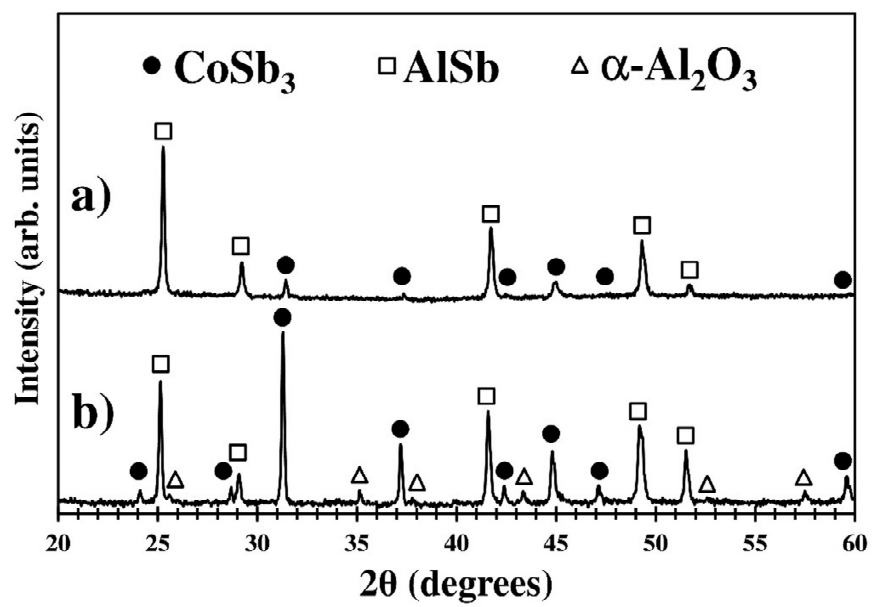


Table 1. Elemental quantifications extracted from the EDS spectra presented in the study

| | Position | at. % of O | at. % of Al | at. % of Co | at. % of Sb |
|---------------|-----------------|-------------------|--------------------|--------------------|--------------------|
| Fig.4 | 1 | 62.2 | - | - | 37.8 |
| | 2 | 50.0 | - | 16.5 | 33.5 |
| Fig.7 | 1 | - | 66.2 | 12.6 | 21.2 |
| | 2 | - | 59.9 | 10.0 | 30.1 |
| | 3 | - | - | 24.7 | 75.3 |
| | 4 | - | - | 25.2 | 74.8 |
| Fig.8 | 1 | - | 68.8 | 12.9 | 18.3 |
| | 2 | - | 63.4 | 11.8 | 24.8 |
| | 3 | - | - | 25.0 | 75.0 |
| | 4 | - | - | 25.1 | 74.9 |
| Fig.10 | 1 | 44.6 | 37.0 | 4.5 | 13.9 |
| | 2 | 41.0 | 27.6 | 4.6 | 26.8 |
| | 3 | - | - | 25.5 | 74.5 |
| | 4 | - | - | 24.9 | 75.1 |
| Fig.11 | 1 | 46.9 | 38.1 | 4.1 | 10.9 |
| | 2 | 43.8 | 26.0 | 4.1 | 26.1 |
| | 3 | - | - | 24.7 | 75.3 |
| | 4 | - | - | 25.2 | 74.8 |

